applied sciences

MDPI

Article

Active Noise Reduction with Filtered Least-Mean-Square Algorithm Improved by Long Short-Term Memory Models for Radiation Noise of Diesel Engine

Semin Kwon [1], Bo-Seung Kim [2] and Junhong Park [1,*]

[1] Department of Mechanical Engineering, Hanyang University, 222 Wangsimni-ro, Seongdong-gu, Seoul 04763, Korea
[2] Samsung Electronics Co., 158 Baebang-ro, Asan-si 31489, Korea
* Correspondence: parkj@hanyang.ac.kr

Abstract: This study presents an active noise control (ANC) algorithm using long short-term memory (LSTM) layers as a type of recurrent neural network. The filtered least-mean-square (FxLMS) algorithm is a widely used ANC algorithm, where the noise in a target area is reduced through a control signal generated from an adaptive filter. Artificial intelligence can enhance the reduction performance of ANC for specific applications. An LSTM is an artificial neural network for recognizing patterns in arbitrarily long sequence data. In this study, an ANC controller consisting of LSTM layers based on deep neural networks was designed for predicting a reference noise signal, which was used to generate the control signal to minimize the noise residue. The structure of the LSTM neural networks and procedure for training the LSTM controller for the ANC were determined. Simulations were conducted to compare the convergence time and performances of the ANC with the LSTM controller and those with a conventional FxLMS algorithm. The noise source adopted sounds from a single-cylinder diesel engine, while reference noises selected were single harmonics, superposed harmonics, and impulsive signals generated from the diesel engine. The characteristics of each algorithm were examined through a Fourier transform analysis of the ANC results. The simulation results demonstrated that the proposed ANC method with LSTM layers showed outstanding noise reduction capabilities in narrowband, broadband, and impulsive noise environments, without high computational cost and complexity relative to the conventional FxLMS algorithm.

Keywords: active noise control; long short-term memory; impulsive noise; diesel engine noise

Citation: Kwon, S.; Kim, B.-S.; Park, J. Active Noise Reduction with Filtered Least-Mean-Square Algorithm Improved by Long Short-Term Memory Models for Radiation Noise of Diesel Engine. *Appl. Sci.* **2022**, *12*, 10248. https://doi.org/10.3390/app122010248

Academic Editor: Yoshinobu Kajikawa

Received: 4 September 2022
Accepted: 9 October 2022
Published: 12 October 2022

1. Introduction

Active noise control (ANC) is a method for removing unwanted noise in a specific area and is based on controlling a second speaker to generate an interference wave. The first patent on ANC was granted to a German engineer in 1936 [1]. Since its first patent, ANC has continually received considerable interest, with numerous related studies conducted. To apply ANC under changing environmental conditions and noise characteristics, a feedforward method has been used to process signals quickly, with adaptive filters used to provide effective responses to changes. A widely used adaptive algorithm for ANC systems is the filtered least-mean-square method [2], derived by Windrow [3]. As shown in Figure 1, a microphone measures a reference noise $x(n)$, and a control speaker generates an interfering wave signal $y(n)$ through an adaptive filter $W(z)$. The noise and control signals are summed over each primary path $P(z)$ and secondary path $S(z)$. The reference noise passes through the primary path and becomes the output noise $d(n)$. The noise residue is measured using an error microphone. The filtered least-mean-square (FxLMS) algorithm performs an adaptation process on the filter $W(z)$, generating $y(n)$ to minimize the noise residue $e(n)$. The LMS algorithm is given as follows:

$$\mathbf{w}(n+1) = \mathbf{w}(n) + \mu e(n)[\mathbf{xs}(n) * \mathbf{x}(n)], \quad (1)$$

where μ is the adaptation step size parameter, $w(n)$ is the adaptive weight vector, $\mathbf{x}(n)$ is the reference noise signal vector, and $\mathbf{xs}(n)$ is the filtered signal from the estimated secondary path filter $\hat{S}(z)$ [2].

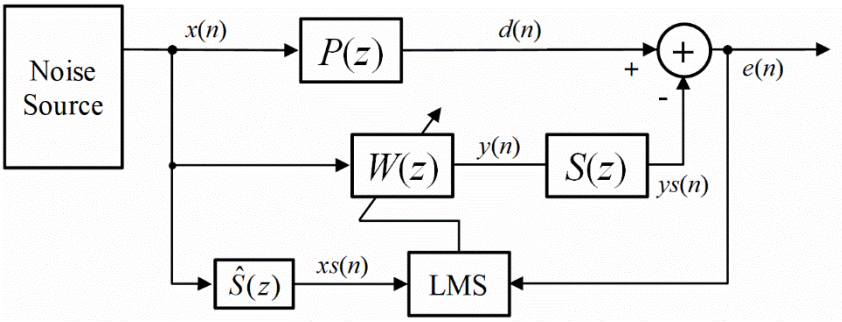

Figure 1. Block diagram of conventional filtered least-mean-square (FxLMS) algorithm based on feedforward active noise cancellation (ANC) systems.

The FxLMS algorithm has been widely used owing to its advantages of low computational complexity, robust performance, and simplicity. The algorithm must converge within a short time to provide efficient noise reduction performance. Many FxLMS algorithms have been proposed with the aim of improving the available convergence conditions and speed [4–6]. Based on theoretical modeling, the necessary and sufficient condition for the convergence of the FxLMS has been derived. In practice, impulsive and multi-tonal noises (which present many difficulties when performing ANC with FxLMS) occur together with the stationary components. A novel secondary path modeling system targeting multiple tonal disturbances has been presented to solve these problems [7]. The ANC performance for impulsive noises has also been enhanced to improve the robustness of FxLMS algorithms [8].

To improve the convergence of ANC, researchers have proposed applying artificial intelligence using neural networks, which have been applied to non-linear ANC to improve their performance [9–11]. Recently, deep neural networks have become a popular field of study and their application range is becoming increasingly diverse. The increased interest in neural networks has led to enhancements in their computational speed, ease of use, and accuracy. Various neural networks have recently been applied in ANC. Zhang et al. used recurrent fuzzy neural networks to propose adaptive non-linear noise-control approaches [12]. Low-frequency noise generated from multi-source railway vehicles was cancelled through a convolution fuzzy neural network [13]. Through the use of a 10-layer extended convolutional neural network (CNN) on a field-programmable gate array, a real-time streaming feedforward ANC system for in-ear headphones was shown in a practical application scenario [14]. A hybrid selective fixed-filter active noise control (SFANC) and filtered-X normalized least-mean-square (FxNLMS) approach was proposed to overcome the adaptive algorithm's slow convergence and provide a better noise reduction level using deep learning [15]. Another study presented a neural-based FxLMS with an error backpropagation algorithm to cancel non-linear broadband noise in an ANC system [16,17]. A multi-layer perceptron was employed in the ANC when the primary path exhibited non-linear behavior [18]. An error backpropagation rule with an adaptive learning rate was applied to update the weight of the neural network. In addition, the functional link artificial neural network filter and its applied algorithm are well-known as effective alternatives to non-linear filters in non-linear ANC systems [19–21]. These non-linear filters using neural network algorithms exhibit complicated architectures and heavy computational costs in implementation, even though the neural network comprises a single layer.

In this study, a multi-layer neural network algorithm based on an alternating FxLMS algorithm is combined with numerical simulations to improve convergence and decrease

noise-canceling errors while avoiding architectural complexity and high computational burdens. The multi-layer neural networks comprise long short-term memory (LSTM) units. In general, the LSTM is specially designed to overcome the limitations of recurrent neural networks (RNNs) when managing long-sequence data. In various synthetic tasks, LSTM can bridge the long time lags between the relevant input and target events [22]. Recently, as hardware performance has increased and the use of software has become simpler, an ANC algorithm through a multi-layer LSTM has become available for processing various types of signals more quickly and accurately over long sequence data. In this study, a method was derived for replacing the deep neural networks from the FxLMS and training procedure of the LSTM. Diesel engine noise was measured under various conditions. The reference noises selected were single harmonics, superposed harmonics, and impulsive signals from the diesel engine. The recorded sound samples were used to compare the noise canceling abilities of the FxLMS and LSTM algorithms. A Fourier analysis was performed on the noise residues to compare and analyze the characteristics and performances of the algorithms. The rest of this paper describes the adaptive filter for the LSTM behavior and the advantages and future tasks of the proposed method.

2. Methods

2.1. Structures of Recurrent Neural Networks for Sequence Data Predictions

The RNN is used to manage the sequence data. As shown in Figure 2, the RNN layer accepts time-varying input data x_t and outputs a value y_t. A loop allows information to be passed from one step of the network to another. The RNN layer H_t derives the output value y_t from the input value x_t at time t and from the weights of H_{t-1}. Simultaneously, the weight information of H_t is conveyed to H_{t+1}. This chain-like characteristic of the RNN shows good performance when processing sequences and lists.

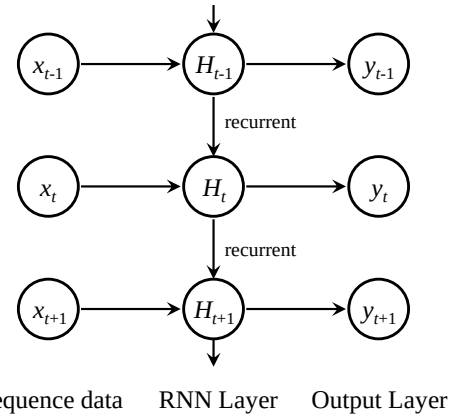

Figure 2. Basic structure of a recurrent neural network (RNN). Chain-like characteristics of RNNs show the advantages of analyzing sequence data.

When processing long-term sequence data using the RNN, errors gradually accumulate from the previous tasks. The LSTM network was developed to avoid the vanishing gradient problem. LSTM networks, as introduced by Hochreiter and Schmidhuber [23], are capable of learning long-term dependencies. LSTM is one of the RNN techniques, and the basic structure is the same as shown in Figure 2. A single LSTM block consists of a cell, input gate, output gate, and forget gate [24]. The LSTM block remembers the values over arbitrary time intervals and the three gates modulate the flow of information into and out of the block. The input gate determines whether data will be stored in the memory cell. The forget gate determines whether the current content of the memory cell must be forgotten. The output gate determines whether the current memory content exhibits the results. Each gate operates according to the following equations.

$$\begin{aligned} \mathbf{i}^t &= \sigma(\mathbf{W}_i \mathbf{x}^t + \mathbf{R}_i \mathbf{y}^{t-1} + \mathbf{b}_i) \\ \mathbf{f}^t &= \sigma(\mathbf{W}_f \mathbf{x}^t + \mathbf{R}_f \mathbf{y}^{t-1} + \mathbf{b}_f) \\ \mathbf{o}^t &= \sigma(\mathbf{W}_o \mathbf{x}^t + \mathbf{R}_o \mathbf{y}^{t-1} + \mathbf{b}_o) \end{aligned} \tag{2}$$

In the above equation, σ is the logic sigmoid used as the gate activation function; $\boldsymbol{x}_t$ is the input vector; **y** is the output vector at time t. **W**, **R**, and **b** are the input, recurrent, and bias weights, respectively. **i**, **f**, and **o** denote the input, forget, and output gate-state vectors, respectively. The cell state $\mathbf{c}_t$ and output of the memory cell $\mathbf{y}^t$ are computed as follows:

$$\begin{aligned} \mathbf{c}^t &= \mathbf{f}^t * \mathbf{c}^{t-1} + \mathbf{i}^t * \tanh(\mathbf{W}_c \mathbf{x}^t + \mathbf{R}_c \mathbf{y}^{t-1} + \mathbf{b}_c) \\ \mathbf{y}^t &= \tanh(\mathbf{c}^t) * \mathbf{o}^t \end{aligned} \tag{3}$$

where $*$ is the scalar product, and **W**, **R**, and **b** are modeling parameters learned during the training of the LSTM layers. The LSTM is capable of processing long-term sequence data owing to the forget gate and output activation function (considered critical components). For fast and stable convergence results, the LSTM neural networks can be trained using stochastic gradient descent and an adaptive learning rate [25]. The characteristics of the LSTM are suitable for predicting input sounds and generating noise-cancelation responses. In this study, deep LSTM neural networks were utilized for ANC to enhance the convergence speed and noise-cancelation capabilities.

2.2. Deep Neural Networks Controller with Long Short-Term Memory (LSTM) for Active Noise Cancellation (ANC) System

A block diagram of the ANC system using the deep neural network filter with the LSTM is shown in Figure 3. Compared to Figure 1, the blocks corresponding to the FxLMS algorithm are replaced with the LSTM controller block. The LSTM controller accepts the noise $x(n)$ as input from the reference microphone. The controller generates an output $y(n)$ that passes through the secondary path $S(z)$ from the input data. An appropriate training set is required to conduct ANC using LSTM. In this study, training sets are created from the ANC results using the fully converged FxLMS algorithm. The output data of the training set consist of one-dimensional time-series data from the $y(n)$ value output when the fully converged FxLMS receives the input $x(n)$. The weights of the LSTM controller are updated using the training sets to minimize the noise residue $e(n)$ when the primary and secondary paths are identical. The LSTM layers used in the ANC in this study consist of two layers containing 128 memory cells each. The fully connected regression layer generates a single value $y(n)$ from the weights of the multiple LSTM layers.

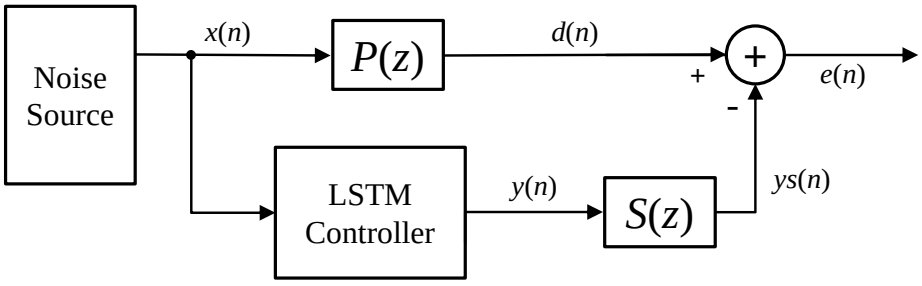

Figure 3. Block diagram of deep neural network filters with long short-term memory (LSTM) for the ANC system. Compared with the conventional FxLMS system, the blocks corresponding to the FxLMS algorithm have been replaced with the LSTM controller block.

3. Simulation Results and Discussion

3.1. Acquisition of Diesel Engine Noise

Engine noise is a major cause of discomfort to vehicle occupants and nearby residents. Vehicles requiring high output power generally use diesel engines, which generate louder noise than gasoline engines. Thus, ANC simulations were conducted to compare the ANC performances of the LSTM controller and FxLMS algorithm to actively reduce diesel engine

sounds. As shown in Figure 4a, the reference noise generated from a 1600-cc single-cylinder diesel engine was recorded by NoiseBook (HDC 45 Noise Gard) when the engine was operated at various RPMs. The microphone for measuring the reference noise was located 2 m back at a height of 1.5 m from the diesel engine, as shown in Figure 4b. The noise was sampled at a frequency of 44,100 Hz. To evaluate the performance according to the adaptive filter algorithm, it was necessary to verify the performance in a wide frequency band and under abrupt modulation noises. In addition, several noisy sounds were measured when the diesel engines were operating at different rotational frequencies and torques to verify the ANC capability of the LSTM controller for broadband noise. The impulsive sound when the diesel engine began operation was also measured. Each recorded sound was used for the ANC simulation.

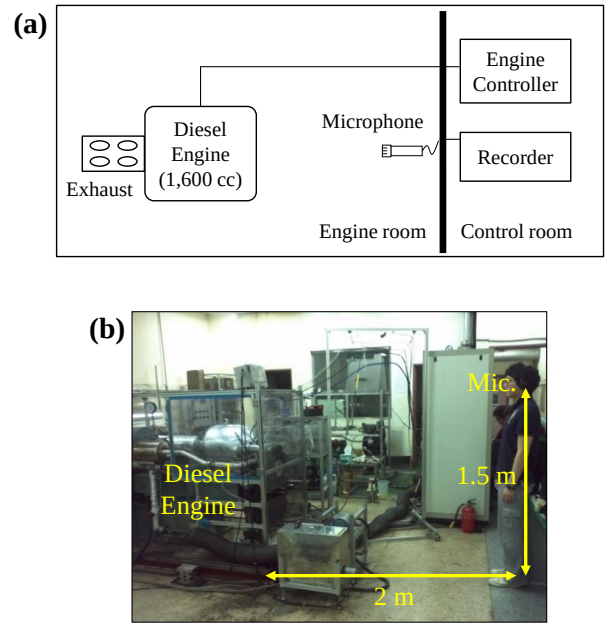

Figure 4. Experimental setup for the reference noise acquisition: (**a**) schematic diagram of the engine and control room and (**b**) 1600-cc single-cylinder diesel engine and measurement location of microphone. The diesel engine operated at various rotational frequencies as the noise signal was measured. The impulsive signal generated when the diesel engine was started was also measured.

3.2. ANC Simulation Results and Discussion

The measured diesel engine sounds at various rotation frequencies were used to train multiple LSTM layers. The noises for the ANC tests comprised completely different fundamental frequencies and situations according to the training set for the diesel engine noises. Each training set consisted of 10 different rotational frequencies of diesel engine noises with a sample size of 200. The multiple LSTM layers were trained for 30 epochs per training set. Parametric studies were conducted to determine the adaptation step size parameter and filter size of the FxLMS algorithm that minimized the noise residue. The filter size was 20 and the adaptation step size was 0.01. The primary and secondary paths were selected as arbitrary filters with lengths of 7. The trained LSTM algorithm was used to actively control the diesel engine noise. The results were compared with those from active control using the conventional FxLMS algorithm. A short-time Fourier transform (STFT) analysis was performed on the noise residue to investigate the characteristics and performance of the algorithm.

The first simulation was used to verify the performance of the harmonics of 60 Hz noise cancellation using the conventional FxLMS algorithm and proposed method with the LSTM neural networks. As shown in Figure 5a, the noise sounds are shown in grey, and the noise residues from the ANC using FxLMS and LSTM are shown in red and blue, respectively. Considering the results of both ANC algorithms for single harmonic sounds,

the conventional FxLMS approach and proposed LSTM controller both eliminate diesel engine noise well during the first 0.6 s. The FxLMS algorithm reaches a noise control level of less than 10% approximately 0.1 s after noise control begins, owing to the convergence. Meanwhile, the LSTM algorithm performs ANC immediately without any convergence time, as the weights of the LSTM units are already determined from the training data. LSTM network predicts the next output data as soon as a fixed number of input data is received in many-to-one mode, so its latency is very short compared to FxLMS. The sampling frequency of the sound samples used in the test is 22,050 Hz, and the output data are predicted with 10 input data, so the latency is 1/4410 s. Because of the characteristics, the LSTM algorithm can directly perform ANC without convergence time. Figure 5b shows the results from the STFT analysis of the noisy data and ANC results. The diesel engine operates at a fundamental frequency of 60 Hz but simultaneously generates various high-frequency components. While performing active control with the FxLMS algorithm, the noise at the fundamental frequency is significantly reduced, but high-frequency noise components remain. When using the LSTM algorithm for ANC, the noise is canceled over the entire frequency range (extremely small intensity of low-frequency components). To compare the noise levels during ANC, the equivalent continuous sound level for each noise was calculated. The equivalent continuous sound level is defined as a sound pressure level that has a total energy equal to the actual fluctuating noise over a given period of time. Thus, the equivalent continuous sound level is in fact the RMS sound level with the measurement duration used as the averaging time. The equivalent continuous sound levels of the original noise, FxLMS, and LSTM approaches are 80.6, 55.1, and 47.7 dB, respectively, thus confirming that the noise reduction of the proposed LSTM algorithm is better than that of the FxLMS algorithm owing to the convergence rate. Figure 5c shows the power spectral density for 0.5~0.6 s, the period in which all ANC algorithms converge. In the case of FxLMS, the low frequency error signal was greatly reduced, but it did not show great performance in the high frequency band. On the other hand, in the case of LSTM, convergence also occurred very quickly and exhibited excellent noise removal performance in all frequency bands. One of the characteristics of LSTM is to predict one output datum that will appear next through several time series input data. Thus, when trained on sounds of the same frequency, the LSTM network can reduce noise in all bands, whether low or high frequencies.

As shown in Figure 6, the simulation used a superposed harmonic noise signal with main frequencies of 33, 35, 50, and 60 Hz measured from a diesel engine. The noise sounds in this simulation were generated by the superposition of each harmonic response. As shown in Figure 6a, the noise control via the FxLMS algorithm achieves a noise level of less than 10% approximately 0.2 s after starting. Compared with the previous active control for the single-fundamental-frequency noise, the convergence of the FxLMS algorithm is delayed owing to the complexity of the reference sounds. The proposed method accomplishes ANC completely, despite the increase in the number of fundamental frequencies of the reference sounds. As shown in Figure 6b, with various fundamental frequencies applied, the noise level in the low-frequency band increases. As a result of the ANC using the FxLMS algorithm, the noise in the low-frequency bands is removed, but the noise components in the high-frequency bands remain. In the case of the LSTM controller, the residual noise increases slightly as the low-frequency noise level increases. All other components in the high-frequency bands are removed. The equivalent continuous sound levels for the original noise, FxLMS, and LSTM are 78.3, 54.9, and 50.9 dB, respectively, confirming that broadband noise is remarkably eliminated by the proposed method, even though the LSTM neural networks were trained only on harmonic signals comprising a single fundamental frequency. As can be seen in Figure 6c, since the superposed harmonic noise signal consists of a high level of low-frequency noise, the low-frequency noise cancellation performance in the period where both FXLMS and LSTM converge is almost similar. Nevertheless, the LSTM performed excellent cancellation in the high frequency band, and the sound

equivalent level was further reduced by about 1.1 dB compared to the FxLMS algorithm in the period 0.5~0.6 s.

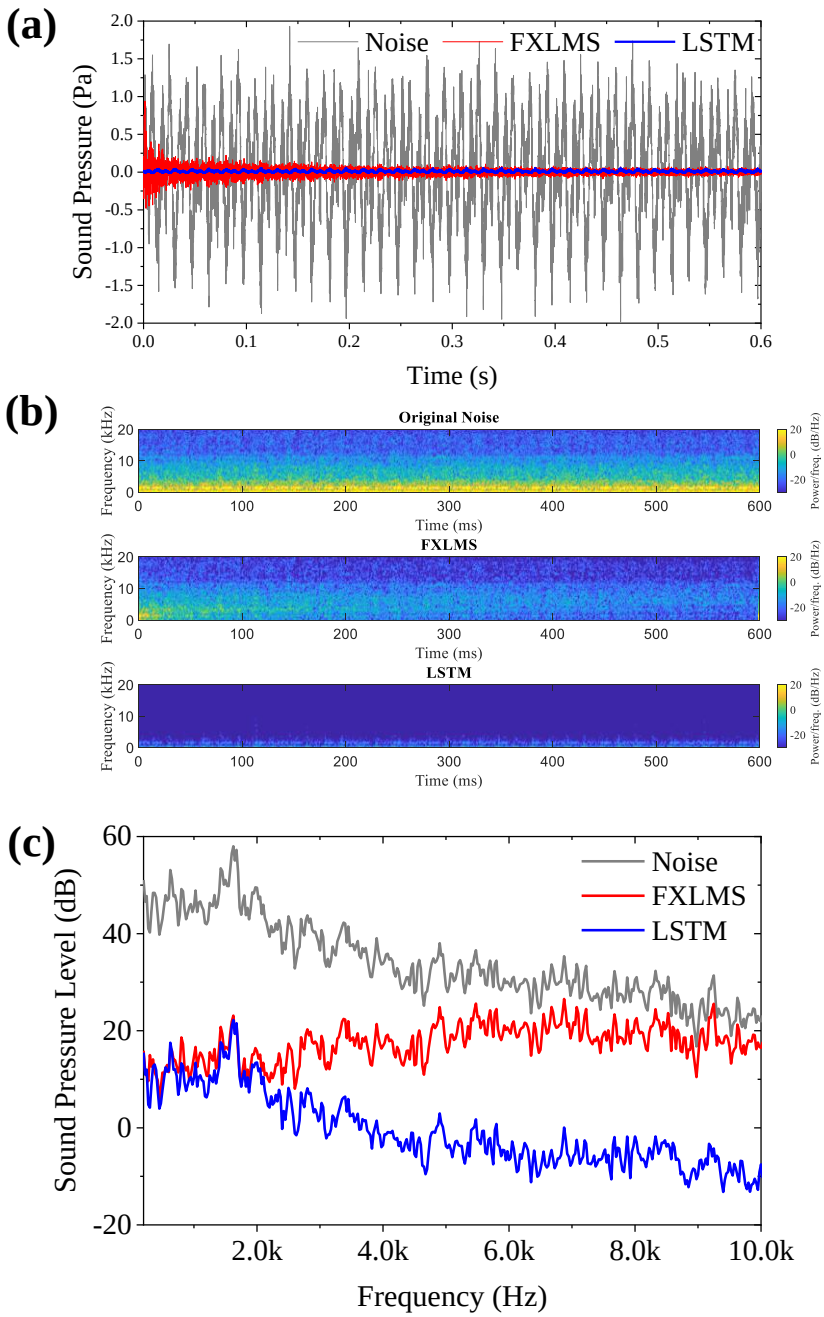

Figure 5. ANC simulation result using FxLMS and LSTM for diesel engine sounds with a main frequency of 60 Hz. (**a**) Time data of the diesel engine noise and ANC results; (**b**) short-time Fourier transform analysis of original noise and noise residue; (**c**) power spectral density of the diesel engine noise and ANC result in the period when the error signal is minimized.

The ANC simulation results for impulsive noises measured during the start-up of the diesel engine are shown in Figure 7. The reference sounds consisted of white noise at 0–1.5 s, and the impulsive sounds owing to the engine started at 1.5–3 s. Steady-state harmonic sounds also contributed to the noise. As shown in Figure 7a, the FxLMS algorithm updates the adaptive filter to converge its weights during 0–1.5 s. When impulsive sounds are generated after 1.5 s, the noise residue of the FxLMS algorithm instantaneously increases again. The adaptation process of the FxLMS is repeated to adjust the weights. At 3 s, the

noise residue of the FxLMS algorithm decreases when the impulsive signal disappears and the harmonic noise is sustained. Through this simulation, it can be confirmed that the FxLMS algorithm shows limited performance for the control of transient sounds. Among the noises occurring in actual situations, impact sounds are the most prominent, as they are difficult to remove through masking or sound absorbers. In contrast, the noise residue of the proposed method (represented by the blue line) has small fluctuations along the amplitude of the reference noise at 1.6, 2.2, and 2.6 s. The LSTM neural networks predict the frequency-modulated signal better than the amplitude modulation. As shown in Figure 7b, the noise level increases overall in all the frequency bands after the engine starts. The FxLMS algorithm does not show good performance for impulsive sound control during engine starts. Approximately 1.5 s after the engine starts, the noise level decreases. However, when ANC is performed using the LSTMs, the noise in the high-frequency band increases slightly, according to the amplitude change of the noise. This increase does not affect performance. The original noise, FxLMS, and LSTM equivalent continuous noise levels for a total of 6 s from white noise to the engine start and steady state are 69.1, 48.2, and 39.8 dB, respectively. The LSTM and FxLMS algorithms show the highest performance compared to the previous simulation results for harmonic signals. Figure 7c shows the power spectral density of noise and ANC results for 3 to 6 s after the ANC algorithm converges. After starting the engine and entering the steady-state, the performance of the two algorithms was similar in the low frequency band as in the previous simulation results, but the performance of the LSTM was better in the high frequency band. The developed algorithm is robust to transient sounds, thus validating that the ANC performance for the impulsive noise from the LSTM controller is also better than that from the conventional FxLMS algorithm.

As a result of the ANC simulations for the noise generated from the diesel engine, the controller of the proposed LSTM neural network shows a performance improvement in terms of convergence and accuracy relative to the conventional FxLMS approach. In practice, noise signals are rarely composed of single-frequency components. Therefore, noise control for impulsive and frequency-modulated noises is essential. The proposed ANC method using the LSTM controller is expected to provide rapid and precise ANC performance for the presented engine sound excitations. Before proceeding with ANC, an appropriate process for training the LSTM layers must be conducted. Recently, training neural networks has become easier and faster as hardware and software performance has increased. The elapsed time for calculating time series output data of length 600 through FxLMS and LSTM in the ANC process using a 3.2 GHz core computer with 16 GB RAM was 0.3486 s and 0.3857 s, respectively. The software used for the analysis was MATLAB R2021a. Through these results, it can be indirectly confirmed that the computational cost does not increase significantly compared to FxLMS, even when deep neural networks composed of LSTM is used.

Although this study only considers diesel engine sounds, LSTM neural networks can contribute to noise reduction in other complex situations, including road and factory environments. Through the proposed algorithm, it was confirmed that the LSTM is capable of noise cancellation for diesel engine noise different from the training data (different fundamental frequency, superposed harmonic sound, engine start noise) in the linear system. Recently, there are various studies on advanced ANC algorithms using deep neural networks [14,15,26,27]. Comparing the performance of advanced ANC algorithms in practical applications is a future task.

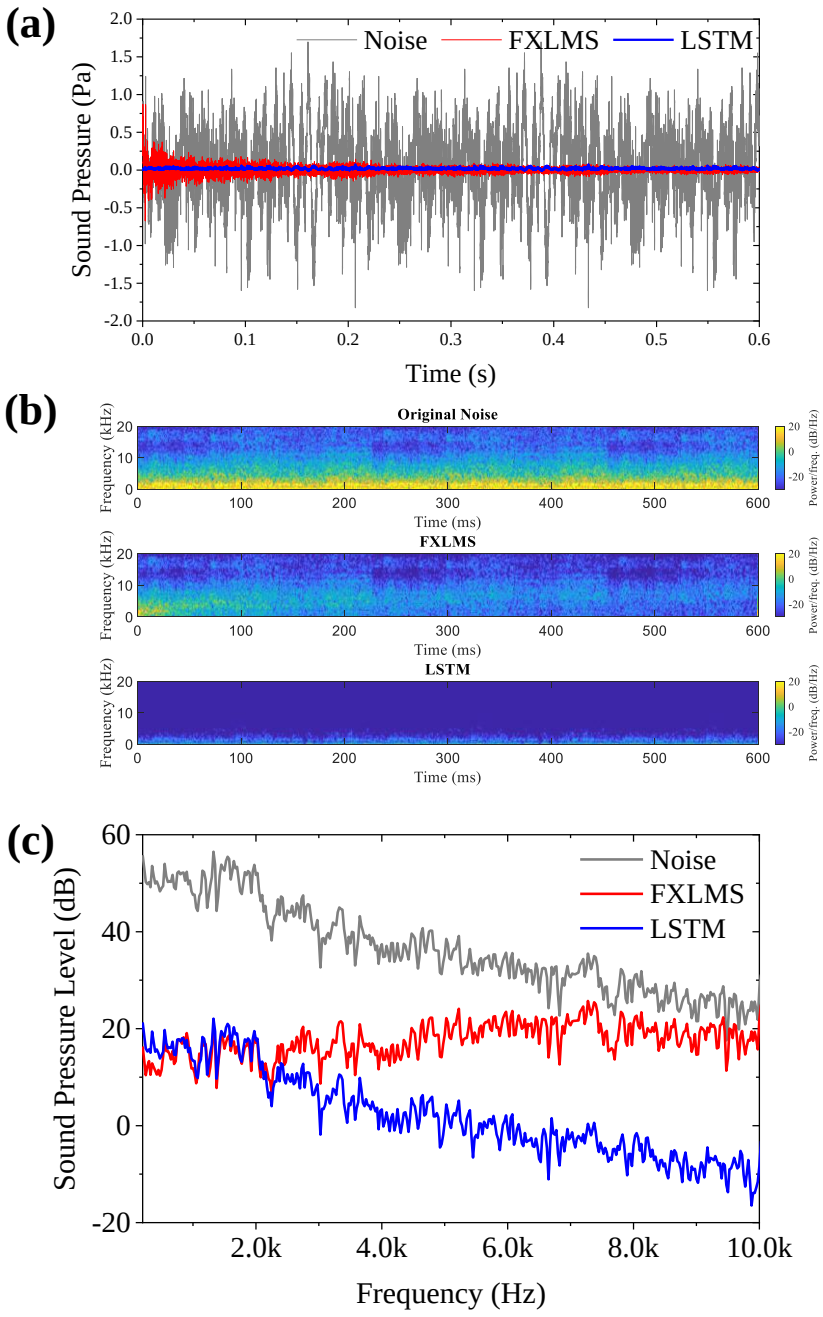

Figure 6. ANC simulation result using FxLMS and LSTM for superposed harmonic sounds with main frequencies of 33, 35, 50, and 60 Hz measured from diesel engines. (**a**) Time data of diesel engine noise and ANC results; (**b**) short-time Fourier transform analysis of original noise and noise residue; (**c**) power spectral density of the diesel engine noise and ANC result in the period when the error signal is minimized.

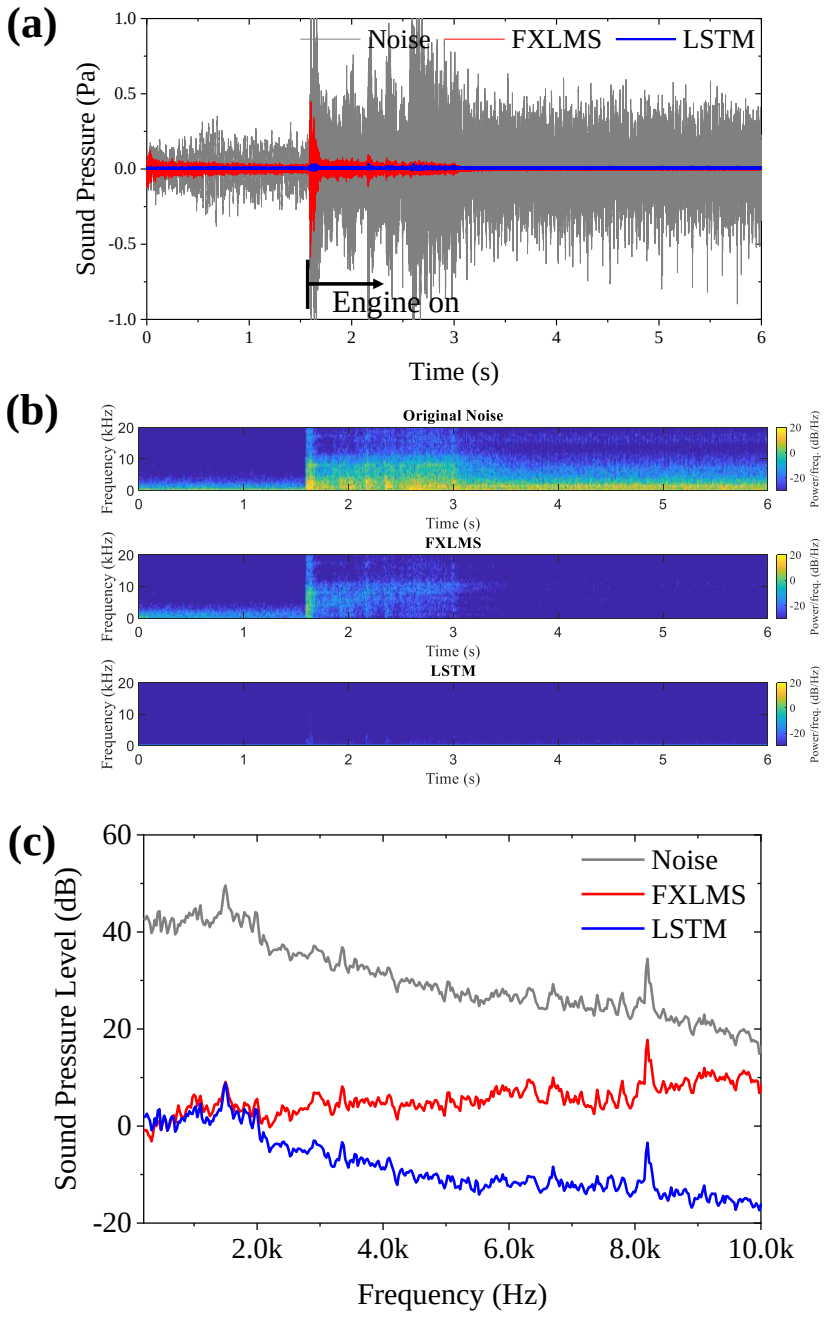

Figure 7. ANC simulation result using FxLMS and LSTM for the impulsive noise signal measured from the start-up of the diesel engine. (**a**) Time data of diesel engine noise and ANC results; (**b**) short-time Fourier transform analysis of original noise and noise residue; (**c**) power spectral density of the diesel engine noise and ANC result in the period when the error signal is minimized.

4. Conclusions

With the advancement of technology, the level of quiet demanded by people in places such as living environments and vehicles has increased. The performance requirements for sound-absorbing materials in products are increasing, and the number of electronic/mechanical systems with ANC technology is rapidly increasing. In particular, artificial intelligence is a promising technology for maximizing noise-cancellation performance.

In this study, LSTM networks were proposed for the ANC algorithm and applied to diesel engine sounds. The LSTM is a recurrent neural network for managing long

sequence data. The ANC controller based on the LSTM layers was suitable for predicting the reference noise and capable of generating the control sounds to minimize the noise residue. The structure of the LSTM neural networks was presented, and the approach to training the LSTM controller for ANC was described. Simulations were conducted to validate the performance of the LSTM controller. Noise samples were acquired from a single-cylinder diesel engine, and the reference noises selected included single harmonics, superposed harmonics, and impulse sounds generated from the diesel engine. For each reference sound, ANC was performed by applying the conventional FxLMS and proposed algorithms. In ANC simulation results, the controller comprising the proposed LSTM neural networks showed performance improvements in terms of convergence and accuracy relative to the conventional FxLMS. In particular, the ANC using the LSTMs for the steady-state harmonic noise converged faster than the FxLMS system. Based on this excellent convergence rate, the overall noise level was significantly reduced. Through the ANC for the superposed harmonics, the proposed algorithm was verified as having excellent performance, even for broadband noise. In particular, the proposed algorithm can control transient sounds. The conventional FxLMS has a disadvantage in that the filter must be re-converged as the signal is modulated. The proposed algorithm showed fast convergence even for the modulated sounds because the training had already been completed. The LSTM network has the advantage of high-frequency noise and transient noise control because it immediately predicted an output when only a fixed number of data was entered. Therefore, the proposed method conducted noise cancellation with robustness in various severely noisy situations, such as in the context of broadband and impulse sounds. Based on these results, LSTM neural networks are considered an appropriate approach to ANC in practical situations.

Author Contributions: Conceptualization, S.K. and J.P.; investigation, S.K. and B.-S.K.; methodology, S.K.; formal analysis, B.-S.K.; project administration, J.P.; resources, J.P.; software, S.K.; supervision, J.P.; writing—original draft, S.K. and B.-S.K.; writing—review and editing, S.K. and J.P. All authors have read and agreed to the published version of the manuscript.

Funding: This work was supported by Korea Institute of Planning and Evaluation for Technology in Food, Agriculture, Forestry (IPET) through Eco-friendly Power Source Application Agricultural Machinery Technology Development Program, funded by Ministry of Agriculture, Food and Rural Affairs (MAFRA) (322047-5).

Institutional Review Board Statement: Not applicable.

Informed Consent Statement: Not applicable.

Data Availability Statement: All data generated or analyzed during this study are included in this published article.

Conflicts of Interest: The authors declare no conflict of interest.

References

1. Lueg, P. Process of Silencing Sound Oscillations. U.S. Patent 2,043,416, 9 June 1936.
2. Kuo, S.M.; Morgan, D. *Active Noise Control Systems: Algorithms and DSP Implementations*; John Wiley & Sons, Inc.: Hoboken, NJ, USA, 1995.
3. Widrow, B.; Stearns, S. *Adaptive Signal Processing*; Englewood Cliffs, Prentice-Hall, Inc.: Hoboken, NJ, USA, 1985; p. 491.
4. Vicente, L.; Masgrau, E. Novel FxLMS convergence condition with deterministic reference. *IEEE Trans. Signal Process.* **2006**, *54*, 3768–3774. [CrossRef]
5. Ardekani, I.T.; Abdulla, W. Theoretical convergence analysis of FxLMS algorithm. *Signal Process.* **2010**, *90*, 3046–3055. [CrossRef]
6. Meng, H.; Chen, S. A modified adaptive weight-constrained FxLMS algorithm for feedforward active noise control systems. *Appl. Acoust.* **2020**, *164*, 107227. [CrossRef]
7. Delegà, R.; Bernasconi, G.; Piroddi, L. A novel cost-effective parallel narrowband ANC system with local secondary-path estimation. *J. Sound Vib.* **2017**, *401*, 311–325. [CrossRef]
8. Akhtar, M.T.; Mitsuhashi, W. Improving performance of FxLMS algorithm for active noise control of impulsive noise. *J. Sound Vib.* **2009**, *327*, 647–656. [CrossRef]

9. Matsuura, T.; Hiei, T.; Itoh, H.; Torikoshi, K. Active noise control by using prediction of time series data with a neural network. In Proceedings of the IEEE International Conference on Systems, Man, and Cybernetics, Vancouver, BC, Canada, 22–25 October 1995; Volume 3, pp. 2070–2075.
10. Pavisic, D.; Blondel, L.; Draye, J.P.; Libert, G.; Chapelle, P. Active noise control with dynamic recurrent neural networks. In Proceedings of the ESANN, Brussels, Belgium, 19–21 April 1995.
11. Bouchard, M.; Paillard, B.; Le Dinh, C.T. Improved training of neural networks for the nonlinear active control of sound and vibration. *IEEE Trans. Neural Netw.* **1999**, *10*, 391–401. [CrossRef] [PubMed]
12. Zhang, Q.-Z.; Gan, W.-S.; Zhou, Y.-L. Adaptive recurrent fuzzy neural networks for active noise control. *J. Sound Vib.* **2006**, *296*, 935–948. [CrossRef]
13. Li, T.; He, Y.; Wang, N.; Jeng, J.; Gui, W.; Zhat, K. Active Noise Cancellation of Rail Vehicles Based on a Convolutional Fuzzy Neural Network Prediction Approach. In Proceedings of the 2021 IEEE Vehicle Power and Propulsion Conference (VPPC), Gijon, Spain, 25–28 October 2021.
14. Jang, Y.-J.; Park, J.; Lee, W.-C.; Park, H.-J. A Convolution-Neural-Network Feedforward Active-Noise-Cancellation System on FPGA for In-Ear Headphone. *Appl. Sci.* **2022**, *12*, 5300. [CrossRef]
15. Luo, Z.; Shi, D.; Gan, W.-S. A Hybrid SFANC-FxNLMS Algorithm for Active Noise Control Based on Deep Learning. *IEEE Signal Process. Lett.* **2022**, *29*, 1102–1106. [CrossRef]
16. Chang, C.-Y.; Luoh, F.-B. Enhancement of active noise control using neural-based filtered-X algorithm. *J. Sound Vib.* **2007**, *305*, 348–356. [CrossRef]
17. Das, K.K.; Satapathy, J.K. New neural network algorithms for nonlinear active noise cancellation with nonlinear secondary path. In Proceedings of the Signal Processing, Communication, Computing and Networking Technologies (ICSCCN), Thuckalay, India, 21–22 July 2011.
18. Krukowicz, T. Active noise control algorithm based on a neural network and nonlinear input-output system identification model. *Arch. Acoust.* **2010**, *35*, 191–202. [CrossRef]
19. Zhao, H.; Zeng, X.; Zhang, J. Adaptive reduced feedback FLNN filter for active control of nonlinear noise processes. *Signal Process.* **2010**, *90*, 834–847. [CrossRef]
20. Sicuranza, G.L.; Carini, A. A generalized FLANN filter for nonlinear active noise control. *IEEE Trans. Audio Speech Lang. Process.* **2011**, *19*, 2412–2417. [CrossRef]
21. Le, D.C.; Zhang, J.; Pang, Y. A bilinear functional link artificial neural network filter for nonlinear active noise control and its stability condition. *Appl. Acoust.* **2018**, *132*, 19–25. [CrossRef]
22. Graves, A. Supervised Sequence Labelling with Recurrent Neural Networks. Ph.D. Dissertation, Technical University of Munich, München, Germany, 2012.
23. Hochreiter, S.; Schmidhuber, J. Long short-term memory. *Neural Comput.* **1997**, *9*, 1735–1780. [CrossRef] [PubMed]
24. Greff, K. LSTM: A search space odyssey. *IEEE Trans. Neural Netw. Learn. Syst.* **2017**, *28*, 2222–2232. [CrossRef] [PubMed]
25. Gers, F.A.; Schraudolph, N.N.; Schmidhuber, J. Learning precise timing with LSTM recurrent networks. *J. Mach. Learn. Res.* **2002**, *3*, 115–143.
26. Park, S.; Patterson, E.; Baum, C. Long Short-Term Memory and Convolutional Neural Networks for Active Noise Control. In Proceedings of the 2019 5th International Conference on Frontiers of Signal Processing (ICFSP), Marseille, France, 18–20 September 2019.
27. Zhang, K.; Lyu, G.; Luo, X. A deep recurrent neural network controller for nonlinear active noise control systems. In Proceedings of the 2020 IEEE 6th International Conference on Computer and Communications (ICCC), Chengdu, China, 11–14 December 2020.